Journal of Alloys and Compounds 519 (2012) 106–111

Contents lists available at SciVerse ScienceDirect

Journal of Alloys and Compounds

journal homepage: www.elsevier.com/locate/jallcom

Influence of superficial CeO_2 coating on high temperature oxidation behavior of Ti–6Al–4V

V. Sreedhar, J. Das*, R. Mitra, S.K. Roy

Department of Metallurgical and Materials Engineering, Indian Institute of Technology, Kharagpur 721302, West Bengal, India

ARTICLE INFO

Article history:
Received 7 November 2011
Received in revised form
21 December 2011
Accepted 22 December 2011
Available online 12 January 2012

Keywords:
CeO_2 coating
Oxidation
Ti–6Al–4V

ABSTRACT

The effect of superficial CeO_2 coating on the oxidation behavior of Ti–6Al–4V has been studied under isothermal and cyclic heating conditions in the temperature range of 923–1223 K in dry air. During the early periods of exposure, the oxide scale grows obeying near linear followed by near parabolic kinetics and consists of alternate layers of α-Al_2O_3 and TiO_2. The mass gain of the uncoated alloys is found to be two times higher than that of the coated one in the temperature range of 923–1123 K up to 36 h of exposure. The scale composition on the bare or coated alloy is found to depend both on the temperature and on the time of exposure. During cyclic exposure, the scale suffers spallation for both the bare and the coated alloy, which has been attributed to insufficient plasticity of the scale.

1. Introduction

High performance materials require stability of the microstructure over a wide range of temperature as well as adequate protection against aggressive environments without losing their strength, ductility and toughness [1]. Ti-based $\alpha+\beta$ alloys, such as Ti–6Al–4V is one of the promising materials, which can not only be used for aerospace applications, but also as a matrix of the SiC fiber reinforced composites for high temperature applications up to about 623 K [2]. On the other hand, near α-alloys such as IM 834, IM 829 can be safely used up to 860 K [3]. Moreover, it has been reported [3] that as the aluminum equivalent (Al_{eq}) in Ti-base alloys increases, the oxidation resistance increases. The possible approaches to increase the upper limit of temperature capability for structural applications of titanium alloys are: (i) strengthening of the conventional titanium alloys by incorporating rare earth elements or rare earth oxide dispersoids [4], (ii) development of alloys based on a fine dispersion of ordered precipitates in a matrix containing either single phase, α or a mixture of α and β phases [5], (iii) development of alloys based on intermetallics, Ti_3Al (α_2) and TiAl (γ) [6], (iv) development of composites based on titanium and/or intermetallic alloys [3] or (v) development of coatings as well as inherently oxidation-resistant alloys [7].

Ti-alloys containing $\alpha+\alpha_2$ phase [5] and dispersions of Ti_5Si_3 silicide [4] have been developed for application in turbo-charger and internal combustion engine components to withstand temperatures up to 1073 K. It is well known that the active/or rare earth elements such as Y, Er, Nd or Gd play a significant role in improving the oxidation resistance, which can be alloyed either during melting [8], or by dispersion of their oxides in the bulk [4]. However, modification of the surface can be achieved either by ion implantation, or by putting overlay coating [7], and thus the use of conventional Ti-alloys with enhanced oxidation resistance can be promoted.

The beneficial effects of superficially applied CeO_2 coating on pure-Fe, Fe–Cr and Fe–Cr–Ni ternary alloys during their high temperature oxidation in reducing the rate of oxidation as well as improving the scale adherence, have already been established through a number of studies [9–11] from this laboratory and also from others [12–14]. However, Fe-based alloys are known to undergo oxidation by outward migration of cations, while the oxide (rutile) scale grown on Ti up to a temperature of 1173 K involves predominant role played by inward diffusion of anions, whereas at higher temperatures outward cationic diffusion is the predominant migration process [15]. Rutile is an n-type semiconductor, but there is no conclusive evidence as to whether interstitial excess cation or oxygen vacancies are the predominant defects in rutile and as such it is reasonable to assume that the outward diffusion of Ti and inward diffusion of oxygen ion both contribute to the diffusion process through the rutile scale during high temperature of oxidation of Ti. Despite the extensive literature available on the effect of reactive elements on the oxidation behavior of Al_2O_3 forming alloys, there is still a remarkable controversy regarding the effects of active elements on the scale growth mechanism as well as improvement in adhesion of Al_2O_3 scales [7].

Accordingly, the present work is aimed at studying the effect of superficial CeO_2 coating on high temperature oxidation behavior of Ti–6Al–4V alloy in the range of 923–1223 K in dry air under

* Corresponding author. Tel.: +91 3222 283284; fax: +91 3222 282280.
E-mail address: j.das@metal.iitkgp.ernet.in (J. Das).

0925-8388/$ – see front matter © 2012 Elsevier B.V. All rights reserved.
doi:10.1016/j.jallcom.2011.12.118

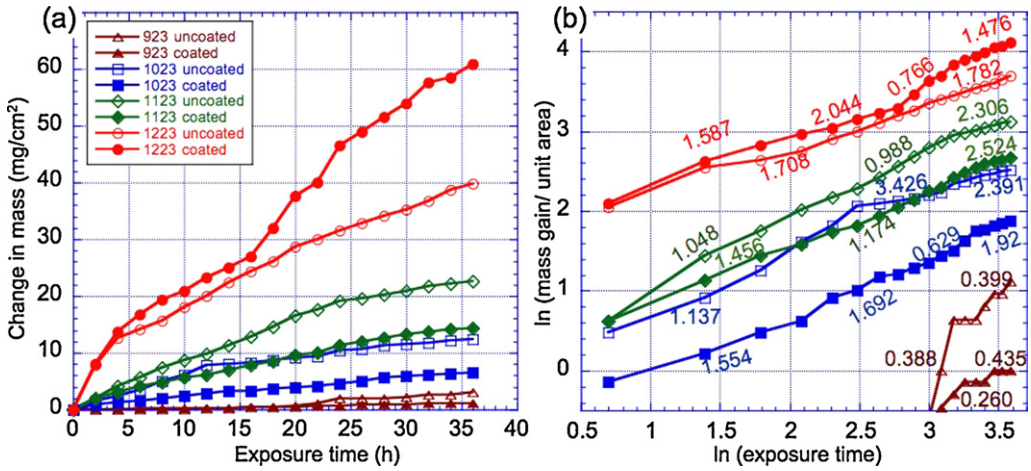

Fig. 1. (a) Plots of change in mass with exposure time during isothermal oxidation of uncoated and CeO_2 coated Ti–6Al–4V alloy in the temperature range of 923 and 1223 K showing beneficial effect of the coating up to 1123 K, and (b) the same data in ln–ln plot showing the dynamic change of the exponent, n during isothermal exposure.

isothermal as well as cyclic conditions. Furthermore, the kinetics of oxide scale growth and the possible growth mechanisms have been investigated and discussed.

2. Experimental

Spectrographic analysis of the selected alloy (Ti–6Al–4V) revealed the composition to be C (0.0079), Si (0.059), S (0.0003), Cr (0.012), Ni (0.019), Al (6.46), V (4.33), Fe (0.038) and the balance Ti. The oxygen, nitrogen and hydrogen contents were estimated to be less than 1445, 194, 37 ppm, respectively. CeO_2 powder of 99.95% purity and −325 mesh size was supplied by Indian Rare Earths Limited, Kerala, India. A slurry was prepared by mixing 5 g of CeO_2 in 100 ml ethanol. In order to obtain a uniform coating thickness, parallelepiped specimens (25 mm × 13 mm × 2 mm) of the alloy were immersed in the slurry after heating at 373 K in an air oven. This process was repeated several times to achieve a continuous scale on surface of the specimen. The volume of CeO_2 deposited per unit area is equals to the ratio of weight gain per unit area and the density of CeO_2. Therefore, the thickness of CeO_2 coating was estimated to be ~0.2 mm. Subsequently, the test specimens were suspended in the hot zone of a vertical tube furnace with the help of a Nichrome wire, which was in turn hung from the weighing pan of a precision balance, so that the mass changes could be measured continuously with an accuracy of ±0.1 mg. The exposure temperature was recorded by using a Pt–Pt/Rh thermocouple kept in the hot zone of the furnace at the closest proximity of the test specimen. Isothermal oxidation tests of the coated and bare alloy were carried out in dry air at 923, 1023, 1123 and 1223 K for 36 h exposure. On the other hand, for cyclic oxidation test, each cycle consisted of heating to 923 K, holding at that temperature for 1 h and subsequently cooling down to room temperature. Both bare and coated alloy samples were subjected to 20 cycles each. The oxide scales formed on different test specimens were characterized by using a Philips PW 1792 X-ray diffraction (XRD) facility with Cu-Kα radiation, and a JEOL JSM 5800 scanning electron microscope (SEM) equipped with Oxford ISIS300 energy dispersive X-ray spectroscopy (EDS) facility. For further post oxidation study, oxidized alloy specimens were sliced perpendicular to the oxidized surface, subsequently mounted and polished before SEM investigation.

3. Results

3.1. Isothermal oxidation kinetics

Fig. 1(a) shows the results related to oxidation kinetics in the form of plots of mass gain per unit area (ΔW) versus time (t) for isothermal oxidation tests carried out at different temperatures on both bare and CeO_2 coated Ti–6Al–4V alloy. Comparison of the plots in this figure leads to the following inferences: (i) the oxidation resistance of the alloy decreases with the increase in exposure temperature; (ii) at 1123 K, the uncoated alloy has gained two times higher mass than that of the coated alloy after exposure for 36 h; and (iii) at temperatures >1223 K, the degradation becomes more severe and appears to be accelerated after exposure for 15 h.

The oxidation kinetics has been quantified in terms of the following power-law relation:

$$\Delta W^n = kt \quad (1)$$

where oxidation exponent, n and the rate constant, k can be determined from the slope and y-axis intercept of the plot of $ln\,\Delta W$ against $ln\,t$. The rates of oxidation of the coated and bare alloy at different isothermal temperatures of exposure can be compared from the values of n and k. Usually $n = 1$ indicates the prevalence of linear oxidation kinetics, while $n = 2$ and 3 imply parabolic and cubic oxidation kinetics, respectively. It is to be noted that higher values of n indicate a slower rate of oxidation, which usually follow either cubic or logarithmic law. Accordingly, the variation of $ln\,(\Delta W)$ with $ln\,(t)$ for various temperatures are plotted in Fig. 1(b), where, the values of n as estimated from the slope of the curves are also shown. Analyses of the results in this figure indicate that the value of n tends to vary with exposure time for a given isothermal test. For example at 1123 K, linear rate of oxidation ($n = 1.048$–0.988) has been noticed up to 30 h of exposure, which is followed by a regime of slower kinetics with $n = 2.306$. Similarly at 1023 K, after a short period of nearly linear rate of oxidation ($n = 1.137$), the kinetics has exhibited $n = 3.426$ during 15–25 h of exposure, which is followed by a regime with $n = 2.391$. However at 1223 K, the oxidation behavior of bare and coated alloy do not exhibit any significant difference, but tend to follow a faster rate ($n = 1.587$–1.782) than that predicted by parabolic law.

The parabolic rate constant (k_p) for each of the isothermal exposure temperature was estimated for both bare and coated alloy by using the following relation:

$$\Delta W^2 = k_p t + C \quad (2)$$

where C is a constant. The values of k_p as obtained from the slope of the ΔW^2 versus t plots, are 0.088 $mg^2\,cm^{-4}\,h^{-1}$ at 923 K and 16.20 $mg^2\,cm^{-4}\,h^{-1}$ at 1123 K in case of bare alloy, while 0.033 $mg^2\,cm^{-4}\,h^{-1}$ at 923 K and 6.295 $mg^2\,cm^{-4}\,h^{-1}$ at 1123 K for the coated alloy. Therefore, the values of parabolic rate constant are almost 2–3 times higher in the case of the bare alloy, than those of the coated alloy indicating a significant reduction in the rate of degradation.

3.2. Cyclic oxidation

The results of cyclic oxidation tests are shown in Fig. 2 depicting the variation in mass gain with number of cycles of exposure.

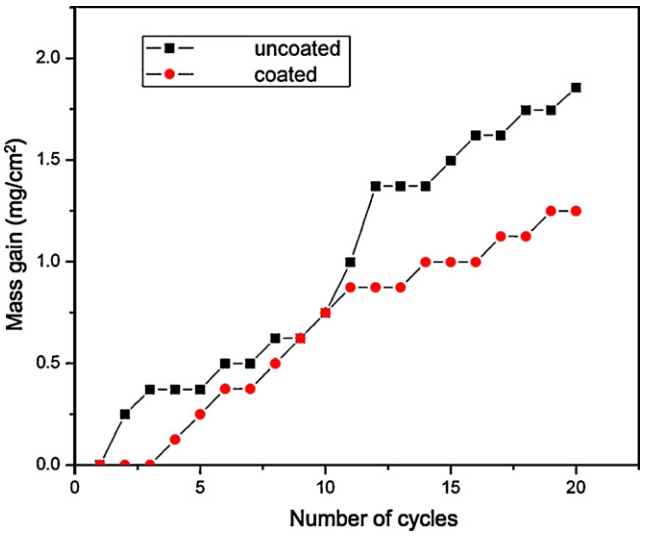

Fig. 2. Plots of mass change for coated and uncoated Ti–6Al–4V alloy during cyclic oxidation up to 923 K.

Analysis of the results in this figure indicates that the net mass gain in the case of bare alloy is ~1.5 times higher than that of the coated alloy while subjected to 20 cycles of exposure at 923 K. The presence of multiple steps in the plots is probably due to scale cracking followed by its healing resulting in an increased mass after short intervals of negligible mass change. Such behavior is suggestive of periodic cracking of the oxide scale, followed by further oxidation. Comparison of the results shows that mass gain after 20 cycles of 1 h exposure at 923 K is greater by 2.48 and 2.50 times for bare and coated alloy, respectively, than that of their isothermal exposure for 20 h at this temperature, as evidenced in Figs. 1(a) and 2.

3.3. Post oxidation studies

The representative XRD patterns of the oxidized bare and coated alloy after isothermal oxidation test at different temperatures are shown in Fig. 3. It can be seen from these patterns that the oxide scale on the uncoated alloy exposed at 1123 K consists of TiO_2 (rutile) and α-Al_2O_3 phases, while AlV_2O_4 also appears to have formed after 36 h of exposure at 1223 K. In case of the coated alloy, the XRD patterns obtained from the oxide scales formed at both

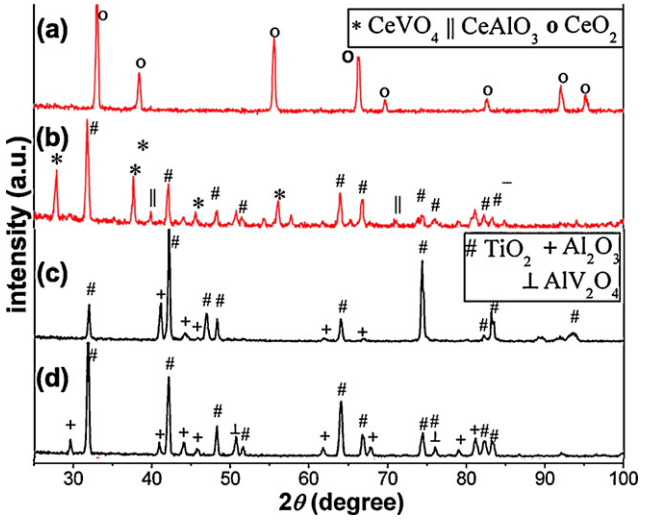

Fig. 3. XRD patterns of the isothermally oxidized coated alloy exposed for 36 h at: (a) 1123 K and (b) 1223 K; and bare alloy at: (c) 923 K and (d) 1223 K.

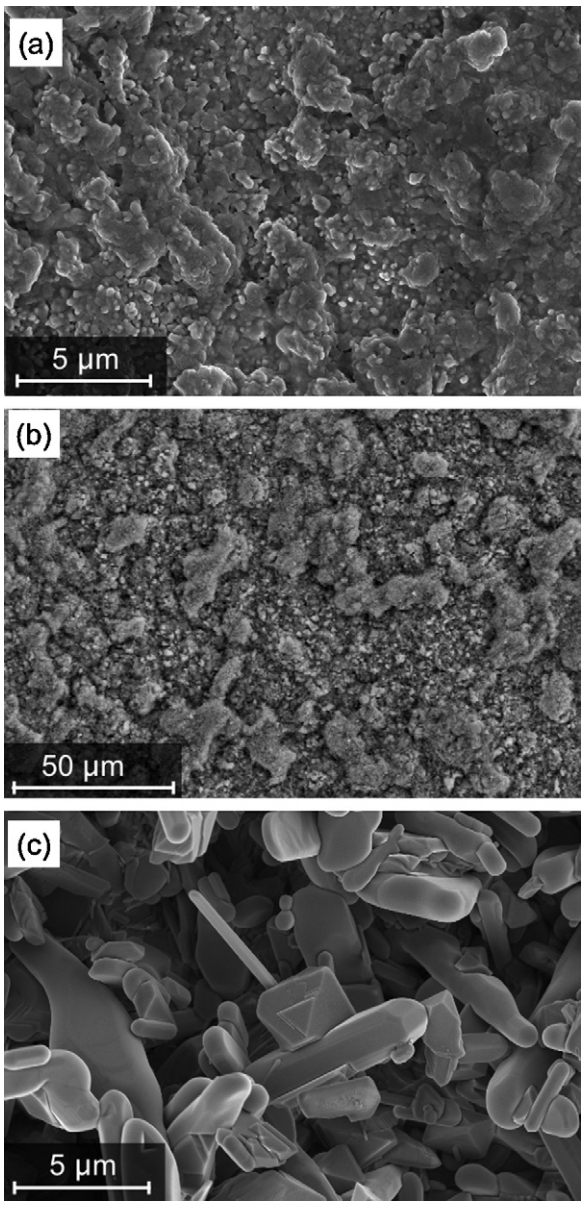

Fig. 4. SEM (SE) images showing the top morphology of oxide layer formed on bare Ti–6Al–4V after exposure for 36 h at: (a) 923 K, (b) 1123 K and (c) 1223 K.

923 K and 1123 K have revealed the existence of only CeO_2, while peaks representing the presence of TiO_2, $CeAlO_3$, $Ce(VO_4)$ phases are found at 1223 K. These observations clearly demonstrate that CeO_2 is thermodynamically stable up to 1123 K, and remains physically adherent to the surface, while its complex oxides are formed during exposure of the coated alloy at 1223 K.

Figs. 4 and 5 show SEM (SE) images depicting the typical top surface morphologies of the scales formed on uncoated and coated alloy, respectively after their isothermal exposure at different temperatures. It is well revealed in Fig. 4(a) that the top outer surface of the scale consists of fine particles having various shapes and morphologies. Such a feature is common for all the bare specimens exposed at temperatures up to 1123 K as shown in Fig. 4(b). Therefore it can be inferred that the rate of growth of the preexisting particles are much higher than the nucleation rate of new particles. However, the top surface scale formed at 1223 K exhibits not only the presence of whiskers with large aspect ratios but also well-developed polygonal particles having diameter of 1–2 μm and length of 3–5 μm, as evidenced in Fig. 4(c). Analyses by EDS has

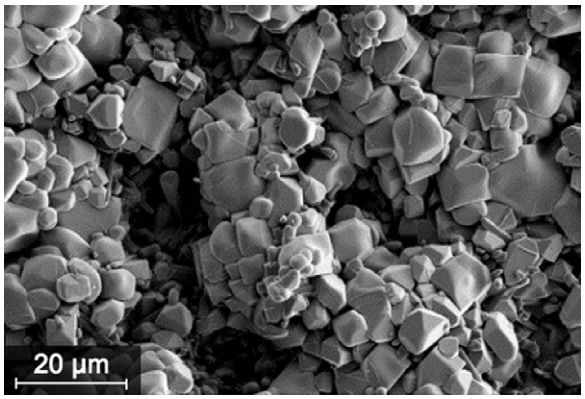

Fig. 5. SEM (SE) image showing the morphology of oxide scale formed on the CeO_2 coated Ti–6Al–4V alloy oxidized at 1223 K for 36 h.

revealed the enrichment of Al and O in the top surface oxide scales formed on the bare alloy exposed in the temperature range of 923–1123 K, which further confirms the presence of α-Al_2O_3 as evidenced in the XRD patterns [Fig. 3(c,d)]. In addition, the presence of TiO_2 (rutile) peaks in the XRD pattern suggests that the Al_2O_3 layer is either very thin or discontinuous in nature. Moreover, the EDS spectrum of the top surface oxide scale formed on the bare alloy at 1223 K, confirms the enrichment of O along with the presence of different elements like Al, V, and Ti indicating that higher temperature promotes the outward diffusion of these elements leading to the formation of α-Al_2O_3, TiO_2, and AlV_2O_4 phases, as identified in the XRD pattern and depicted in Fig. 3(d).

In the case of coated alloy exposed at 1223 K, the microstructure of the top oxidized surface exhibits the presence of 2–5 μm cube shaped particles, which form 20–30 μm size clusters, as shown in Fig. 5. Analysis of this oxide scale by EDS has confirmed the presence of elements such as Ce, Al, V, and Ti along with oxygen, which is suggestive of the formation of their respective oxides.

The results of SEM and EDS examinations carried out on the alloy/oxide scale cross-sections of bare and coated alloy are shown in Figs. 6 and 7, respectively. The scales formed on both bare and coated alloy appear to posses a multilayered structure, where the layers with different compositions can be visually distinguished from one another as shown in Figs. 6(a) and 7(a). Examination of the EDS X-ray maps, for the bare oxidized alloy [Fig. 6(b–e)], reveals the

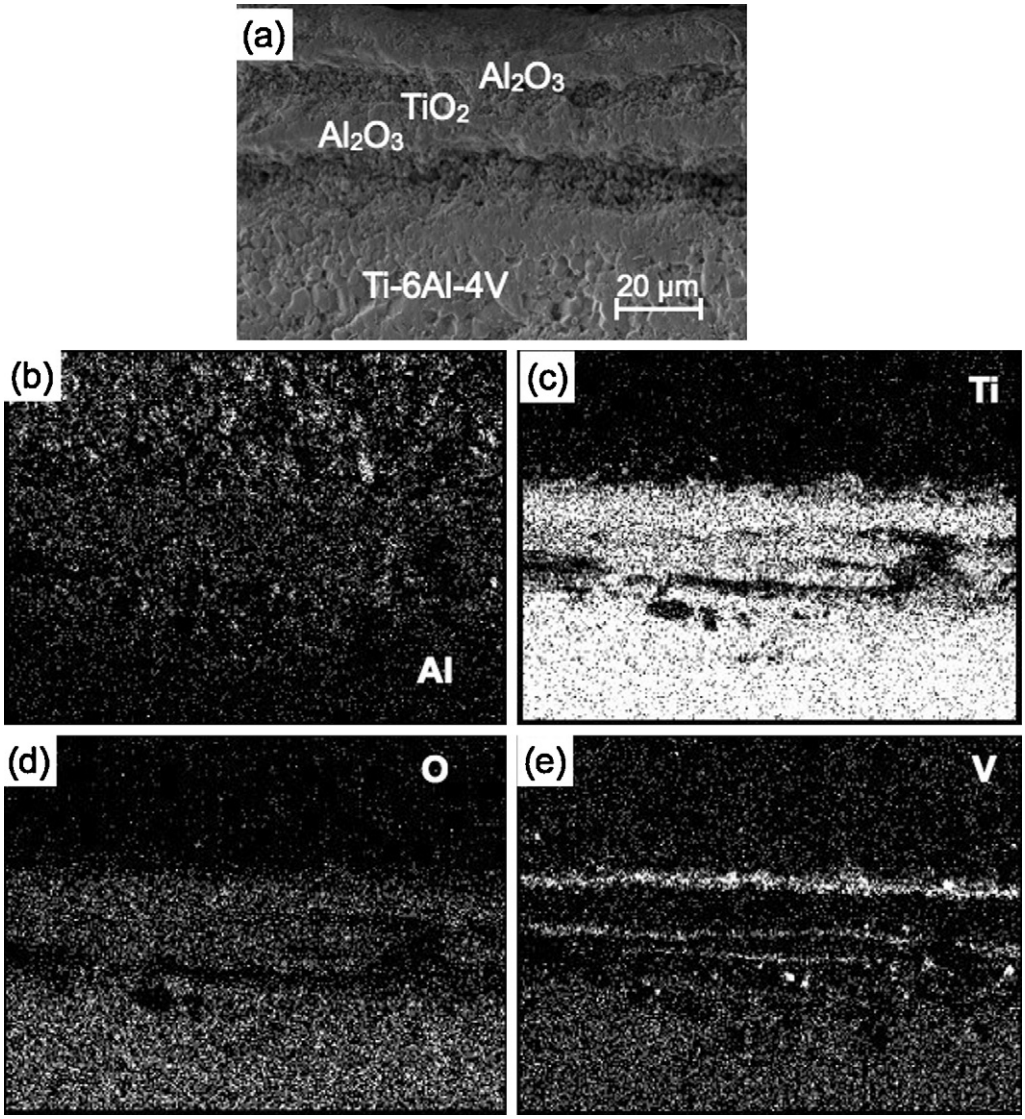

Fig. 6. (a) SEM (SE) image of the alloy/scale cross-section, and EDS X-ray maps of; (b) Al (c) Ti (d) O, and (e) V showing typical compositional profiles of the scale formed on bare Ti–6Al–4V alloy isothermally oxidized at 1123 K for 36 h.

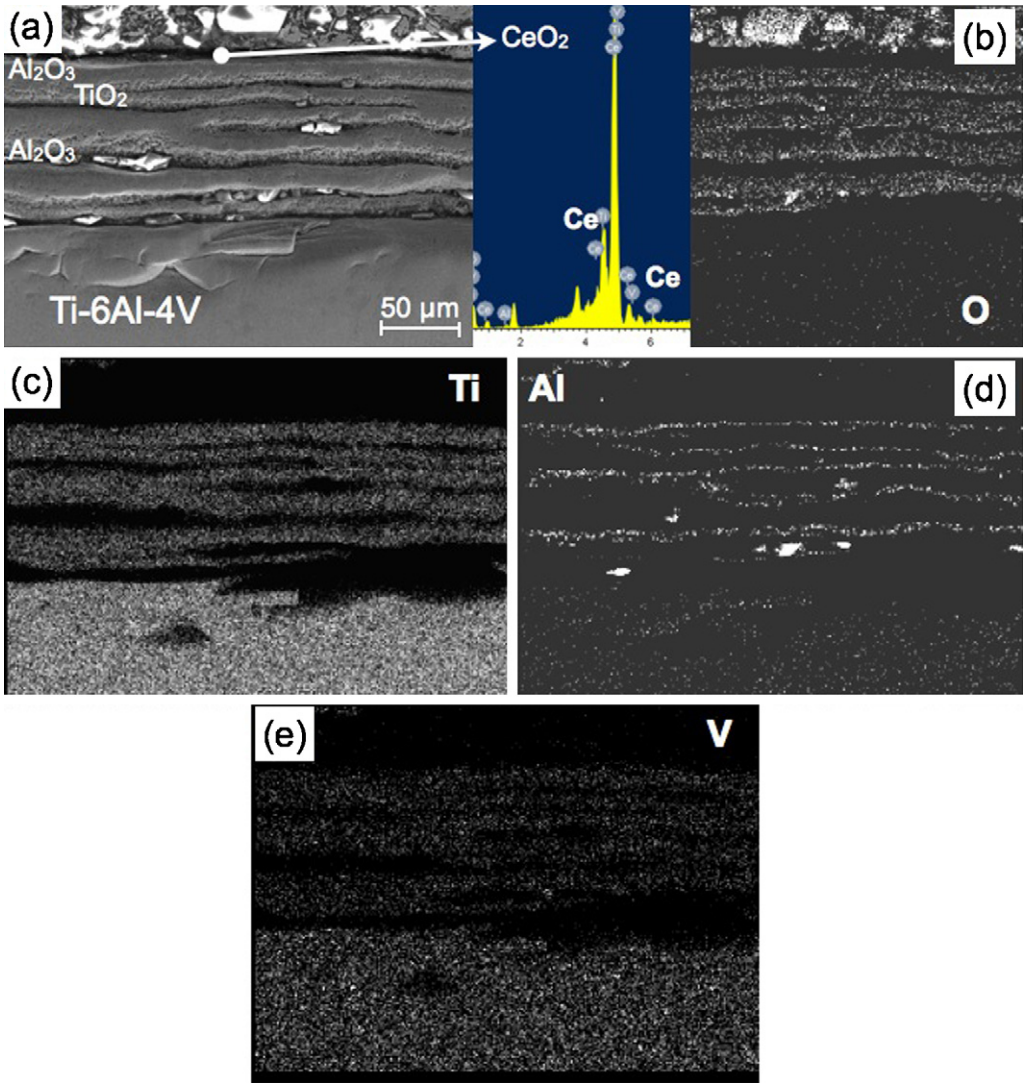

Fig. 7. (a) SEM (SE) image of the alloy/scale cross-section, and EDS X-ray maps of (b) O (c) Ti and (d) Al, and (e) V showing typical compositional profile of the scale formed on coated Ti–6Al–4V alloy after oxidation at 1123 K for 36 h. Inset (a) and (b) showing the EDS spectra confirming the presence of CeO_2 layer on the top of the oxidized coated alloy.

outermost layer to be Al_2O_3, followed by alternate layers Al_2O_3 and TiO_2, with a vanadium-rich oxide layer at the Al_2O_3/TiO_2 interfaces. On the other hand, the EDS X-ray maps [Fig. 7(b–e)] for the elemental distributions in the oxide scale formed on the coated alloy show similar features as that for the bare alloy, with the exception of a 2–4 μm thick top CeO_2 layer. XRD investigation [Fig. 3(a)] has also confirmed the presence of CeO_2 on the surface of specimens after 36 h exposure in air up to 1123 K. However, V could not be traced in the oxide scales of the coated specimens exposed up to 1123 K. The thickness of TiO_2 layers has been estimated to vary between 5 and 10 μm. While thickness of Al_2O_3 layer varied between 2 and 4 μm and these layers are found to be rather discontinuous revealing the presence of interfacial cracks or discontinuities between the alternate oxide layers. On careful examination of the SEM images of the alloy/oxide scale cross-sections, formed at different temperatures, it is found that the number and the thickness of the different oxide layers increase with increase in the temperature of exposure. Formation of such alternate layers of TiO_2 and Al_2O_3 can only be possible by the outward diffusion of both Al^{3+} and Ti^{4+} ions through the preexisting TiO_2 or Al_2O_3 layers, respectively, as reported earlier [16]. Even though XRD analysis has revealed the formation of AlV_2O_4 only at 1223 K, but diffusion of V from the base alloy and nucleation of AlV_2O_4 at the interface of Ti-/Al-oxides appears to have occurred at even lower temperatures.

4. Discussion

The frequent changes in the oxidation exponent (n) as described in Fig. 1(b) suggest that the growth of the oxide scales on both bare and coated Ti–6Al–4V alloy have taken place through multiple steps. The results for the oxidation of this alloy in air at 923 K and 1123 K have demonstrated that Al_2O_3 and TiO_2 layers have grown alternately and leading to the formation of an oxide scale possessing a multilayered structure for both coated and uncoated conditions. Furthermore the thickness and the number of such layers increase with the increase of exposure temperature. Such observations in the case of a Ti–6Al–4V alloy have already been demonstrated by Du et al. [16] and the suggested mechanism also seems to be valid in the present study. At the initial stages of oxidation, it is possible to accommodate the growth related internal stresses between the oxide scale and substrate by its plastic flow.

At relatively lower temperatures of exposure, the diffusion of the alloying elements is rather slower than that at higher temperature, the oxide scale consists of relatively thinner oxide layers. However, the thickness of individual layer increases with time and due to the limited plasticity of the oxide scale, cracks are formed between the oxide scale and substrate, when a critical thickness of the oxide scale is exceeded. The stress caused during cooling from the temperature of exposure to room temperature by the mismatch in expansion coefficients between the oxide scale and substrate can be released by cracking initially at the edges of the alloy and then progressively expanding through the entire surface. Formation of such cracks is expected to bring about a change in the kinetics of isothermal exposure, and eventually lead to spallation when exposed for much longer periods. The detachment at the scale substrate interface would decrease outward diffusion of Ti and Al ions, while oxygen will still diffuse inward favoring condition for the formation of a second TiO_2 layer. On the other hand, cyclic oxidation study has revealed that the alloy in both bare and coated conditions could withstand thermal shock up to 20 cycles only at 923 K. But experiments conducted at higher temperatures have shown that significant spallation occurred even after first cycle, because of relatively higher magnitude of thermal stresses compared to those developed on cyclic exposure at 923 K or lower temperatures.

The CeO_2 coating has been found to substantially improve the isothermal oxidation resistance of the Ti–6Al–4V alloy up to 1123 K, while the microstructure of the oxidized alloy beneath the superficial coating appears to be more or less the same as that of the uncoated alloy, indicating that the oxidation mechanism remains unaltered. It is reported that the presence of rare-earth oxide such as CeO_2 in which oxygen defect is predominant, inward diffusion of oxygen ions is faster than the outward diffusion of cations [17]. In the present study, superficial ceria coating acts as an inert marker. The presence of CeO_2 at the outer most layer of the oxide scale of the coated oxidized alloy (Fig. 7), without any wrinkling of the outer surface of the scale, suggest that the oxidation has progressed by inward transport of oxygen. In such a case, a sound adhesion of the oxide scale to the substrate is expected to be achieved. The diffusion coefficient of O^{2-} anion is reported to be $9.55 \times 10^{-9}\ m^2\ s^{-1}$ in CeO_2, $2.88 \times 10^{-5}\ m^2\ s^{-1}$ in Ti and $4.6 \times 10^{-3}\ m^2\ s^{-1}$ in Al in the temperature range of 1100–1200 K [18]. Therefore, CeO_2 acts as a kinetic barrier to the scale growth process. However, growth of TiO_2 scale on Ti–6Al–4V is accomplished by oxygen ingress below 1123 K, whereas above this temperature, migration of Ti interstitial predominates as reported earlier [2]. At 1223 K, CeO_2 gets dissociated, promoting the outward diffusion of V through the Ti-/Al-oxide layers in order to form the complex oxide, AlV_2O_4. Therefore, the protective scale of Al_2O_3 is consumed, causing accelerated oxidation at this temperature.

5. Conclusions

Application of a superficial coating of CeO_2 decreases the rate of oxidation of Ti–6Al–4V up to 1123 K under isothermal condition. The oxide scale on the bare alloy consists of alternate layers of Al_2O_3 and TiO_2. Both number and thickness of these layers increase with the increase in temperature and exposure time. The CeO_2 coating acts as a barrier to the ingress of oxygen and outward diffusion of Ti, Al and V, which in turn lowers their activities thereby retarding formation of their respective oxides. The coated alloy could well withstand thermal shock up to 20 cycles. However, at higher temperatures, complex Ce-based compounds are formed due to its reaction with other oxides of alloying elements like Al, V and severe spallation occur failing to accommodate the generated stress.

Acknowledgments

The authors thank A. Pariya, S. Mondal and B. Das of the Central Research Facility at IIT Kharagpur for technical help. Financial support provided by Defense Research Development Organization, New Delhi, India, and SRIC, IIT Kharagpur on ISIRD scheme (UEC) are gratefully acknowledged.

References

[1] E.A. Brandes, G. Brook, Smithells Metals Reference Book, Butterworth-Heinemann, Bodmin, UK, 1992.
[2] P. Kofstad, P.B. Anderson, O.J. Krudtaa, J. Less-Common Met. 3 (1961) 89–97.
[3] A.K. Gogia, Defence Sci. J. 55 (2005) 149–173.
[4] H. Nagai, Mater. Sci. Forum 43 (1989) 75–130.
[5] G. Lutjering, S. Weissmann, Acta Metall. 18 (1970) 785–796.
[6] A.K. Gogia, T.K. Nandy, D. Banerjee, T. Carisey, J.L. Strudel, J.M. Franchet, Intermetallics 6 (1998) 741–748.
[7] E. Lang, The Role of Active Elements in the Oxidation Behaviour of High Temperature Metals and Alloys, Elsevier, London, U.K, 1989.
[8] A.G. Paradkar, A.V. Rao, A.K. Gogia, Trans. Indian Inst. Met. 53 (2000) 231–242.
[9] S.K. Mitra, S.K. Roy, S.K. Bose, Oxid. Met. 39 (1993) 221–229.
[10] S. Seal, S.K. Bose, S.K. Roy, Oxid. Met. 41 (1994) 139–178.
[11] S.K. Roy, C. Bottino, V. Rakesh, S. Kuiry, S.K. Bose, ISIJ Int. 35 (1995) 433–442.
[12] R. Haugsrud, Corros. Sci. 45 (2003) 1289–1311.
[13] S.M.C. Fernandes, O.V. Correa, L.V. Ramanathan, J. Therm. Anal. Calorim. 106 (2011) 541–543.
[14] S. Strauss, H.J. Grabke, Mater. Corros. 49 (1998) 321–327.
[15] P. Kofstad, High-temperature Oxidation of Metals, John Wiley & Sons Inc., New York, USA, 1966.
[16] H.L. Du, P.K. Datta, D.B. Lewis, J.S. Burnell-Gray, Corros. Sci. 36 (1994) 631–642.
[17] U.K. Chatterjee, S.K. Bose, S.K. Roy, Environmental Degradation of Metals, Marcel Dekker Inc., USA, 2001.
[18] R. Freer, J. Mater. Sci. 15 (1980) 803–824.